Journal of Magnetism and Magnetic Materials 347 (2013) 61–67

Contents lists available at ScienceDirect

Journal of Magnetism and Magnetic Materials

journal homepage: www.elsevier.com/locate/jmmm

Abnormal temperature dependence of the coercive field in FePt thin films

J.M. Guzmán [a], N. Álvarez [b], H.R. Salva [b], M. Vásquez Mansilla [b], J. Gómez [b], A. Butera [b,*,1]

[a] Facultad de Ciencias Químicas – Universidad Nacional de Córdoba – 5000 Córdoba, Argentina
[b] Centro Atómico Bariloche (CNEA), Instituto Balseiro (U. N. Cuyo) and Conicet, 8400 Bariloche, Río Negro, Argentina

ARTICLE INFO

Article history:
Received 7 May 2013
Received in revised form
15 July 2013
Available online 2 August 2013

Keywords:
FePt
Thin films
Magnetic anisotropy
Critical thickness
Strain induced anisotropy

ABSTRACT

We have observed notable changes in the magnetic response of FePt thin films that we have attributed to a transition in the magnetic domain structure when the film thickness or the temperature is varied. The critical thickness for this transition depends on the Q-factor, $Q = K_\perp / 2\pi M_s^2$, so that a change in the domain structure is expected when changes in the perpendicular anisotropy, $K_\perp$, or the saturation magnetization, M_s, occur. At room temperature these samples have $Q \sim 0.3$, and a transition between planar to stripe-like domains occurs for a film thickness $d \sim 30$ nm. Due to the different thermal expansion of the FePt alloy and the Si substrate a reduction in Q is predicted when the temperature is lowered. From magnetization vs. field loops measured at different temperatures below $T = 300$ K, we have effectively observed a change in the coercive field which can be associated to a transition from stripe-like to in-plane domains. The transition temperature range is broad, indicating a gradual variation between the two magnetic configurations, but changes systematically with film thickness, consistent with an interfacial induced stress. A model that includes the temperature dependence of the strain and the magnetization, predicts correctly the observation of a larger critical thickness at lower temperatures.

1. Introduction

FePt alloys of equiatomic composition form in an equilibrium thermodynamic phase of tetragonal symmetry (the chemically ordered fct structure called $L1_0$) which has been extensively investigated in the last years due to the increasing interest in ultrahigh coercivity materials in the magnetic recording industry. This system shows one of the largest known magnetocrystalline anisotropies [1–5] that can be larger than 7×10^7 erg/cm^3. Most applications of this alloy are in the form of thin films which tend to grow in a metastable cubic crystalline phase displaying relatively soft magnetic properties [1,6,7]. The saturation magnetization of both crystalline phases is almost the same. Due to the potential technological impact the vast majority of the research was devoted to the high anisotropy alloy and less attention was paid to the so-called A_1 soft magnetic phase.

We have recently reported in a series of works [8–10] in which we have characterized the structural and magnetic properties of FePt thin films at room temperature that they tend to grow with a [111] texture normal to the film plane and with a compressive in-plane stress. These two effects contribute to the appearance of an anisotropy perpendicular to the film plane, in the case of texture because the [111] is an easy axis for the magnetocrystalline anisotropy and in the case of stress because the negative deformation and the positive magnetostriction coefficient also favor a perpendicular axis of anisotropy.

The competition between the effective perpendicular anisotropy, $K_\perp$, that tends to align the magnetization in the out of plane direction, and the shape anisotropy, that in the case of a thin film favors the in-plane alignment, determines not only the equilibrium orientation of the magnetization vector, but also the structure of the magnetic domains. The ratio between the perpendicular anisotropy energy and the demagnetizing term defines the quality factor, $Q = K_\perp / 2\pi M_s^2$. Depending on the value of Q and the film thickness it is possible to find: (i) a magnetic domain configuration consisting of in-plane planar domains, (ii) a periodic array of stripes with an out of plane component of the magnetization which alternates between the "up" and "down" directions or, (iii) for $Q > 1$, a bubble-like structure in which the magnetization in each region is completely perpendicular to the film surface. The structure of stripe magnetic domains can only be found in films in which there is a component of the magnetic anisotropy perpendicular to the film plane (i.e. $Q > 0$) and was previously reported in a large number of metallic ferromagnetic materials such as Co [11], FePd [12,13], Co_3Pt [14], or Permalloy ($Fe_{20}Ni_{80}$) [15,16].

For $Q < 1$ the transition from planar to stripe domains occurs above a critical thickness d_{cr} that depends on the material properties

* Corresponding author. Tel.: +54 294 4445100.
E-mail address: butera@cab.cnea.gov.ar (A. Butera).
[1] Instituto de Nanociencia y Nanotecnología, Argentina.

0304-8853/$ - see front matter © 2013 Elsevier B.V. All rights reserved.
http://dx.doi.org/10.1016/j.jmmm.2013.07.037

such as the anisotropy, the saturation magnetization and the exchange stiffness constant. There are several models for the calculation of d_{cr} (see for example Refs. [17–19]) that predict larger values of d_{cr} in materials with a large magnetization, a large exchange, or a small anisotropy. Research in materials in which stripe domains are observed reported values of the critical thickness in the range of 20–30 nm for Co [11], partially ordered FePd [20] or disordered FePt films [8], and significantly larger values (of the order of 200 nm) in films with a lower anisotropy, such as Permalloy [16].

Although FePt thin films grow with a [111] texture [8] which could induce an out of plane anisotropy of magnetocrystalline origin, we have observed in a set of films with the same crystallographic texture but a different degree of stress [21] that the magnetic properties change significantly, indicating that the main contribution to the perpendicular anisotropy is due to magnetoelastic effects.

If changes in the stress of the films can be induced, it would then be possible to study the dependence of the critical thickness d_{cr} with the perpendicular anisotropy. The anisotropy, and consequently the Q factor, can be varied for example by changing the temperature of the films. The different thermal expansion coefficients of the Si substrate and the FePt film produces an interfacial induced strain which affects the perpendicular anisotropy and modifies the Q factor. In this work we report a study of the variation of the critical thickness for the formation of stripe domains as a function of temperature in a set of FePt films and develop a simple model that explains the observed behavior.

2. Experimental details

Details of the samples used in this work can be found in Ref. [8]. Briefly, FePt films have been fabricated by dc magnetron sputtering on naturally oxidized Si (100) substrates from an FePt alloy target with a nominal atomic composition of 50/50. Eight different films with thicknesses of: 9, 19, 28, 35, 42, 49, 56 and 94 nm were deposited at room temperature. The magnetization data were measured using either a LakeShore model 7300 VSM or a Quantum Design SQUID with maximum fields of 1.2 and 5 T and lower temperature limits of $T=80$ and 4 K, respectively. Images of the magnetic domains were obtained at room temperature with a Veeco Dimension 3100 AFM/MFM with Nanoscope IV electronics. Magnetic images have been acquired using medium moment, medium coercivity tips (MESP) from Bruker.

3. Experimental results and discussion

3.1. Magnetic force microscopy and magnetization measurements

The whole set of films was studied by MFM at room temperature. We have found that films with thicknesses below 28 nm exhibit a very limited number of magnetic domains even in the maximum available scan area of $100\times100\ \mu m^2$ (see Fig. 1). In a remanent saturated state domain walls for $d\leq28$ nm could be only observed close to the edges of the samples, where closure domains are generally formed. If the film is in a demagnetized remanent state it is possible to find "cross tie"-like domain walls in different regions of the sample, as shown in Fig. 1(a). As can be observed in Fig. 1(c), measurements of the magnetization as a function of magnetic field in the plane of the film show a large squareness and remanence, which is a strong indication that the magnetization in these samples stays essentially in the film plane, and also makes more difficult the observation of domain walls. The coercive field is relatively small, with values below 20 Oe for $d\leq19$ nm and $H_c\sim40$ Oe for $d=28$ nm.

Films with a thickness $d\geq35$ nm present a completely different magnetic behavior. In these samples the MFM measurements at remanence show a periodic structure in the form of stripes (top right panel of Fig. 1), which generally occurs when the magnetization vector presents an oscillating component perpendicular to the film plane. The corresponding hysteresis loop [Fig. 1(d)] has a linear part at low fields, as expected for this kind of magnetic domain structure. This linear variation of M between $H=0$ and the in-plane saturation field $H_{S\parallel}$ is related to the alignment of the out of plane component of M with the external field. The value of $H_{S\parallel}$ depends on $K_\perp$, M_s and d [8]. In films thicker than d_{cr} the remanent magnetization tends to decrease [8] when the film thickness increases suggesting that the out of plane component of M becomes larger. The coercive field in the thicker samples is always much larger ($H_c\gtrsim120$ Oe) than the values found for $d<d_{cr}$ ($H_c<40$ Oe), due to the changes occurring in the domain structure. We would like to stress that the correlation between MFM images and H_c shown in Fig. 1 was found in the whole set of samples

As our MFM can only operate at room temperature, we have used the fact that there is a close correlation between the magnetic domain structure and the hysteresis loops. The more sensitive experimental parameter to distinguish between both types of domains is the coercive field and has then been used in this study as a signature for the presence or absence of stripes in the samples.

In Fig. 2 we show M vs. H loops for the samples of 42 and 94 nm at three different temperatures between 80 K and 300 K. It can be observed that in the case of the thicker sample the hysteresis loop does not change significantly in this temperature range. In fact the loops remain almost the same, except for a gradual increase of the coercive field and a reduction of the in-plane saturation field. These observations suggest that for this film the stripe structure is preserved down to 4 K, the lowest analyzed temperature. In the case of the 42 nm sample the behavior is considerably different. When lowering the temperature from 300 K the coercive field first increases and at around 240 K it starts to decrease, giving quite similar loops for $T=200$ K and 300 K. However, at lower temperatures the linear part of the loop almost disappeared and H_c was reduced to approximately one half of the high temperature value.

In order to get a deeper understanding of this complex magnetic behavior, we measured the coercive field as a function of temperature for the whole set of samples. Results, presented in Fig. 3, show for some thicknesses the expected increase in H_c when the temperature is lowered, but for samples with $35\ \text{nm}\leq d\leq56$ nm an unusual behavior can be observed. These films have a maximum in the coercivity for a certain temperature and then a notorious decrease is found when the samples are cooled to lower temperatures. At very low temperatures H_c tends to increase again. There are a few works describing the temperature dependence of the coercivity in FePt alloys, but they only discuss the behavior of the ordered $L1_0$ phase. Both in the cases of nanoparticles [22] or thin films [23] it was found that H_c decreases continuously for higher temperatures, as usually happens in ferromagnetic materials. There is a report [24] in highly textured thin films of an anomalous decrease in H_c below room temperature, which was ascribed to the exchange interaction between crystals oriented with their easy axis parallel or perpendicular to the film plane. Although the coercivity in films generally depends on extrinsic factors, such as the number or density of pinning sites for domain wall pinning, when studying the temperature dependence of coercivity in ferromagnets two limiting cases are often encountered: particle-like and continuous film-like behaviors. The former case applies to magnetically isolated small particles in which the energy to overcome the barrier for magnetic reversal is provided thermally. A temperature dependence of the form $H_c=H_{c0}[1-(T/T_B)^{1/2}]$, with H_{c0} the coercivity at $T=0$ K and T_B the blocking temperature, is predicted for particles of identical size [25].

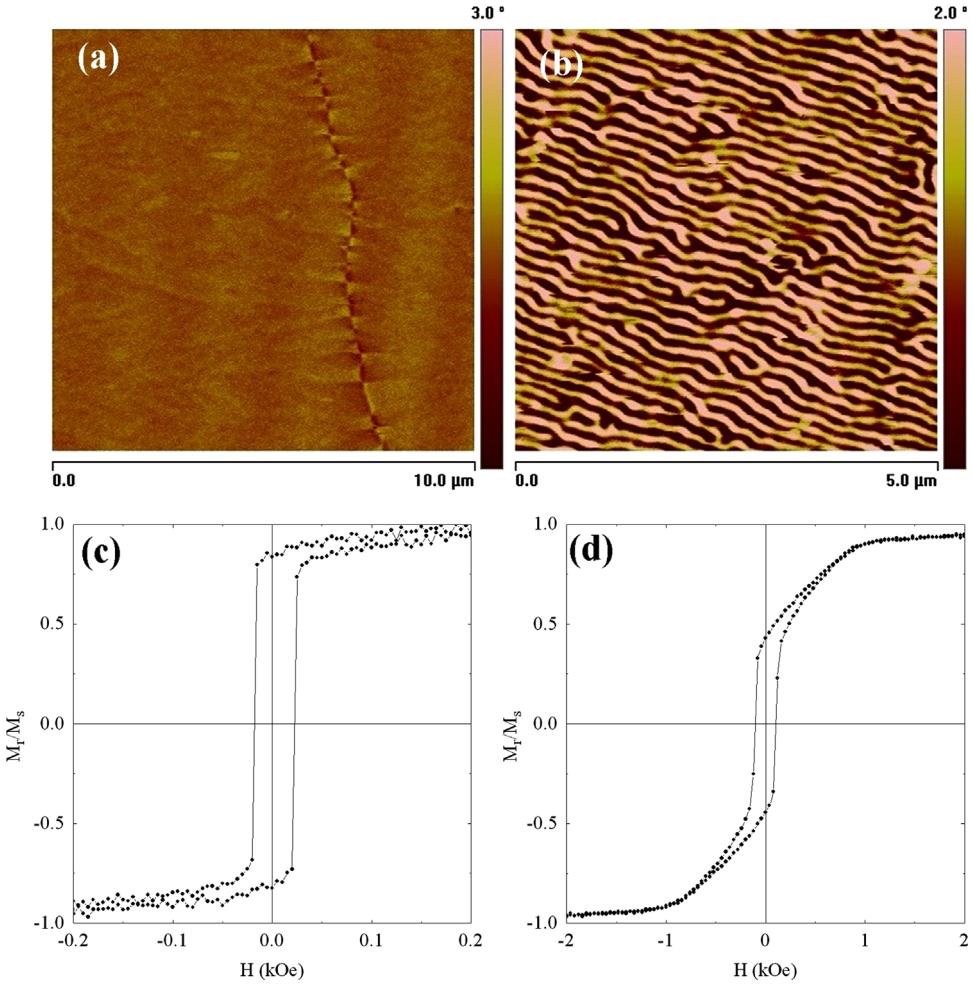

Fig. 1. MFM images of two films with a thickness of 19 nm (a) and 94 nm (b). The *x*-scale is indicated in the figure and is similar to the *y*-scale. The color coded vertical bar represents the phase shift of the cantilever resonance. The domain wall in the thinner film with the cross tie structure was observed after demagnetizing the sample in a rotating and decreasing field. In the other case the domain structure corresponds to the remanent state obtained after saturating the sample with a magnetic field of 1 kOe applied outside the microscope. The corresponding in-plane hysteresis loops in the bottom panel (c and d) show the change in the magnetic behavior of the films according to their thickness. Note the different field scale and the larger remanence in the thinner film. (For interpretation of the references to color in this figure caption, the reader is referred to the web version of this article.)

The other case applies to continuous films where the ferromagnetic domain walls are pinned by a random array of inhomogeneities [26]. Depending on the unpinning process "strong" or "weak" pinning situations can be found that differ also in the activation energy required to unpin a domain wall. For strong pinning the coercivity decreases (due to thermal activation effects) as T increases following the law $H_c = H_{c0}[1-(T/T_S)^{2/3}]^2$. For weak pinning the relationship between coercivity and temperature is linear, $H_c = H_{c0}[1-(T/T_W)]$, T_S and T_W stand for the characteristic temperatures where the pinning effect vanishes. As expected for thermally activated models, the reversal of the magnetization is assisted by the thermal energy and hence a decrease in H_c is always predicted when T increases. This behavior is found in most magnetic materials (see for example Refs. [27–29]) and the cases in which a decrease in H_c at lower temperatures is found are usually a consequence of factors such as phase transformations [30], exchange coupling in systems of two (or more) phases [31], or competing magnetic anisotropies [24].

As we have already mentioned, in our films we have two competing anisotropies that above a certain thickness favor the formation of a stripe structure with a relatively large coercivity. Results shown in Fig. 3, in which H_c has a maximum value at a given temperature, and decreases for lower values of T, suggest that samples in the range $35\ \text{nm} \leq d \leq 56\ \text{nm}$ present stripes above a certain temperature, T_{sp}, and planar domains below it. Because of the relatively broad temperature range of the transition, the definition of this "stripe to planar" characteristic temperature is somewhat arbitrary, but we have used as a convention to assume that stripe domains cease to exist when the coercive field starts to decrease. Other conventions could have been used (for example the middle point between the maximum and the minimum of H_c) but they are harder to define in some of the curves. In any case it should be kept in mind that this value of T_{sp} is an upper limit for the transition in the domain structure. The values of T_{sp} for the different samples have been indicated with arrows in Fig. 3 and have been plotted in Fig. 4 with solid symbols. Although no decrease in H_c was observed for the sample with $d = 94$ nm, we have plotted a point with an open symbol at $T = 0$ K to indicate that for this thickness planar domains are predicted to exist only at negative temperatures.

3.2. Model for the estimation of the critical thickness as a function of temperature

The curve that gives the critical thickness for the transition from planar to stripe domains as a function of the Q-factor has been deduced in Refs. [18–20]. The simplified model of Refs. [19,20] is essentially one dimensional. It assumes that the magnetization vector can point only in a plane perpendicular to

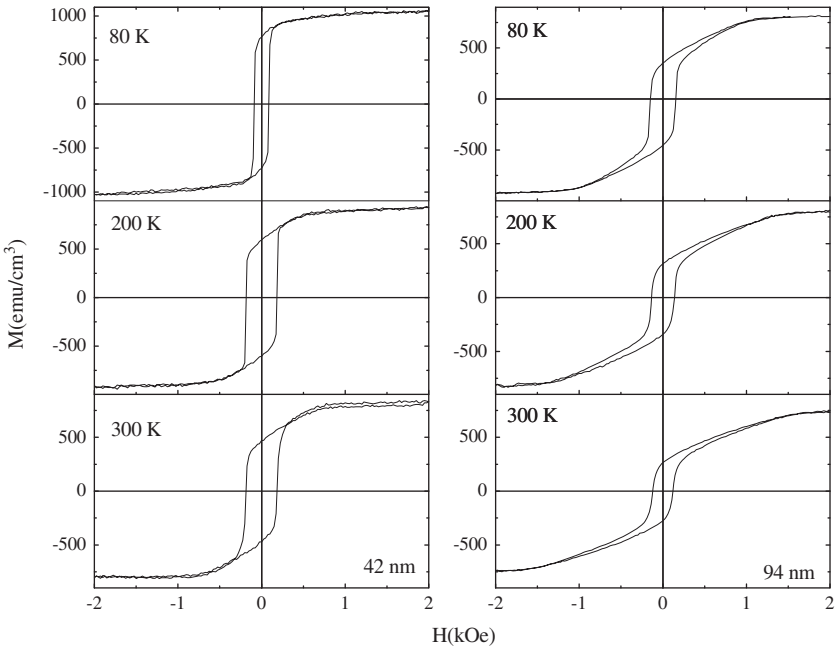

Fig. 2. Magnetic hysteresis loops at different temperatures for $d=42$ nm (left) and $d=94$ nm (right). For the thinner film the coercive field starts to decrease below $T\sim 240$ K, while for $d=94$ nm it increases monotonically when T is lowered. The field where saturation in the magnetization is observed decreases at lower temperatures in this sample.

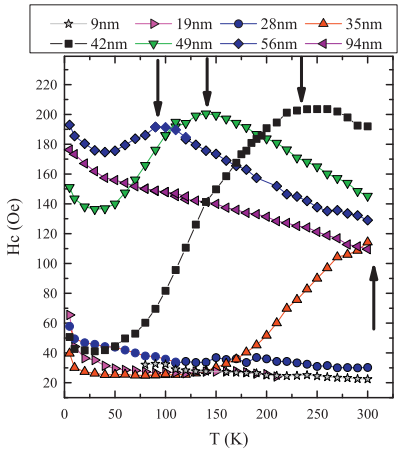

Fig. 3. Temperature variation of the coercive field for the complete set of samples. The vertical arrows indicate the temperature where H_c starts to decrease. Note that for the films with $d\leq 28$ nm or $d\geq 94$ nm the coercivity always increases when the temperature is lowered.

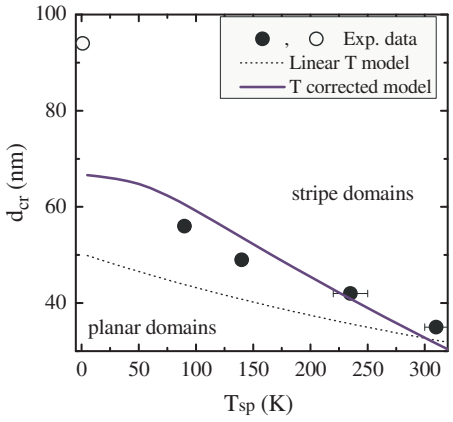

Fig. 4. Phase diagram of the critical thickness as a function of the temperature that separates the regions of planar and stripe domains. We show the predictions for the "linear" model in which the only temperature dependence is in the thermal expansion, and the full model in which changes in all relevant parameters due to temperature variations have been considered. We also plotted the datum for $d=94$ nm at $T=0$ K (with an open circle), even though this film shows a continuous increase of H_c with temperature and the transition to planar domains is not observed in the region of positive temperatures.

the film surface that contains also the direction of alignment of the stripes, with a gradually alternating out of plane component. The magnetization angle changes periodically in this plane with a period that increases with the film thickness. A very convenient closed form to describe the Q dependence of the critical thickness can be obtained from the following pair of parametric equations [19,20]:

$$Q=\frac{K_\perp}{2\pi M_s^2}=\frac{1}{2\pi}\left[3x-(\pi+3x)e^{-\pi/x}\right]$$

$$d_{cr}=d_l\frac{\sqrt{2}\pi^{3/2}}{x}[x-(\pi+x)e^{-\pi/x}]^{-1/2}. \quad (1)$$

In the above expression the exchange length is defined as $d_l=\frac{1}{2}\sqrt{A/(2\pi M_s^2)}$, with A the exchange stiffness constant. As discussed in the paper of Murayama [18] the one dimensional model predicts in general a critical thickness that is larger than the observed value. To obtain a more reliable value of d_{cr} as a function of Q it is then necessary to consider that the angle of the magnetization vector can vary within the film thickness and can also have an in-plane component perpendicular to the direction of the stripes. In this situation the problem becomes considerably harder from the mathematical point of view because there are no simple closed expressions for the critical thickness as a function of Q. We have plotted in Fig. 5 the numerical results from Fig. 3 of Ref. [18] and the one dimensional analytical curve from Eq. (1). It can observed that both models predict almost the same dependence, at least for $Q\lesssim 0.4$. Note, however, that the factor $\frac{1}{2}$

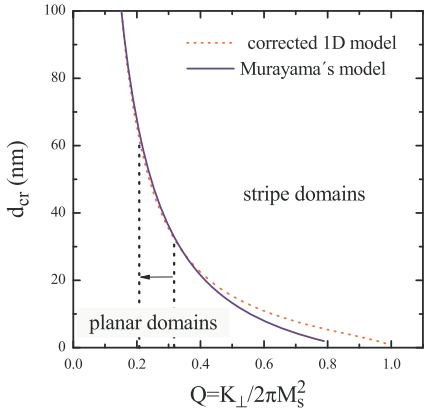

Fig. 5. Critical thickness as a function of $Q=K_\perp/2\pi M_s^2$ obtained from the parametric Eqs. (1) (dotted line) and from the paper of Murayama (continuous line) [18]. The two vertical lines indicate the Q values at room temperature ($Q\sim0.32$) and at $T=4$ K ($Q\sim0.21$). It can be observed that a reduction of Q produces an increase in the critical thickness for the observation of stripe domains.

in the exchange length was not in the original work of Refs. [19,20] and was added here in order to match the critical thickness predicted by the model with that observed in our samples. We also show in Fig. 5 how a reduction in Q produces a relatively fast increase in the critical thickness for the observation of stripes.

The temperature dependence of Q may arise from the anisotropy $K_\perp$ or from the magnetization M_s. We have analyzed both contributions to see how they influence the critical thickness. We have considered first the temperature variation of $K_\perp$, assuming that, as already mentioned in the introduction section, the major contribution is due to the different thermal expansion between the FePt thin film and the Si substrate. In a simple model in which a biaxial stress (σ) is present in the film plane of a [111] textured sample, the perpendicular anisotropy may be written [32] as

$$K_\perp = K_{\perp 0} - \tfrac{3}{2}\lambda_{111}\sigma, \tag{2}$$

with $K_{\perp 0}$ the induced perpendicular anisotropy at room temperature due to residual stresses (and possibly a minor magnetocrystalline contribution due to the [111] texture in the films) and λ_{111} the magnetostriction constant. The saturation magnetostriction constant of FePt disordered films was reported by Aboaf et al. [33] ($\lambda=70\times10^{-6}$), and more recently by Spada et al. [34] ($\lambda=34\times10^{-6}$). There are also reported values in FePd films by Shima et al. [35] ($\lambda=65\times10^{-6}$) and Wunderlich et al. [36] ($\lambda=250\times10^{-6}$, in films prepared at 423 K). Note that in all cases the reported magnetostriction is positive. For our estimation we use the average room temperature value of $\lambda_{111}=\lambda\sim50\times10^{-6}$, and extrapolated a linear behavior to low temperatures. To our knowledge, the temperature dependence of λ in disordered FePt thin films has not been measured and the only available data correspond to bulk FePd alloys [37]. In this system $\lambda=49\times10^{-6}$, 48×10^{-6}, and 41×10^{-6} for $T=4$, 77, and 300 K, respectively. Assuming the same temperature variation for λ in FePt we obtain $\lambda=60\times10^{-6}$, and 58.5×10^{-6} for $T=4$ and 77 K, respectively.

The temperature dependence of the biaxial stress in the case of a film–substrate interface may be approximately expressed [38–40] as

$$\sigma(T)=\frac{\varepsilon(T)E_{\mathrm{FePt}}(T)}{1-\nu(T)}\simeq\frac{(\alpha_s(T_0)-\alpha_f(T_0))(T-T_0)E_{\mathrm{FePt}}(T_0)}{1-\nu(T_0)}, \tag{3}$$

with ε the strain, E Young's modulus, α_s and α_f the coefficients of thermal expansion of the substrate and the film, respectively and ν Poisson's ratio. This expression is valid in the case of a uniformly stressed film in which the relaxation at grain boundaries may be neglected, and gives an upper limit for the strain in the samples. The linear temperature behavior in the above formula is only valid in a limited temperature range around T_0 (in this case $T_0\sim300$ K) in which the variables α, E and ν are assumed to have a negligible temperature dependence. However, it is well known that both the thermal expansion α and Young's modulus E_{FePt} do vary if the temperature interval is very large. In order to consider the full temperature dependence of Eq. (3) we have assumed the same temperature dependence for α as for the phonon specific heat, within the Einstein model, and hence the strain is given by

$$\begin{aligned}\varepsilon(T)&=\int_{T_0}^{T}(\alpha_s(T)-\alpha_f(T))\,dT\\&=\int_{T_0}^{T}\left(\alpha_0^{\mathrm{Si}}\left(\frac{\theta_E^{\mathrm{Si}}}{2T}\right)^2\frac{1}{\sinh^2\left(\frac{\theta_E^{\mathrm{Si}}}{2T}\right)}-\alpha_0^{\mathrm{FePt}}\left(\frac{\theta_E^{\mathrm{FePt}}}{2T}\right)^2\frac{1}{\sinh^2\left(\frac{\theta_E^{\mathrm{FePt}}}{2T}\right)}\right)dT\\&=\alpha_0^{\mathrm{Si}}\theta_E^{\mathrm{Si}}\left(\coth\frac{\theta_E^{\mathrm{Si}}}{2T}-\coth\frac{\theta_E^{\mathrm{Si}}}{2T_0}\right)\\&\quad-\alpha_0^{\mathrm{FePt}}\theta_E^{\mathrm{FePt}}\left(\coth\frac{\theta_E^{\mathrm{FePt}}}{2T}-\coth\frac{\theta_E^{\mathrm{FePt}}}{2T_0}\right).\end{aligned} \tag{4}$$

If we use the reported [41] values of the thermal expansion coefficients (close to room temperature) for silicon [100] substrates, $\alpha_s=2.5\times10^{-6}$ K^{-1}, and for FePt films, $\alpha_f=10.5\times10^{-6}$ K^{-1}, we end up with $\alpha_0^{\mathrm{Si}}=3.2\times10^{-6}$ K^{-1} and $\alpha_0^{\mathrm{FePt}}=11.05\times10^{-6}$ K^{-1}. The Einstein temperatures θ_E^{Si} and θ_E^{FePt} may be obtained from the Debye temperatures of Si ($\theta_D=645$ K), Fe ($\theta_D=470$ K) and Pt ($\theta_D=240$ K) using the relation $\theta_E/\theta_D\sim(\pi/6)^{1/3}$. For FePt there are no reported values of θ_D so we used the simple model that estimates the Debye temperature of an alloy from θ_D of the composing elements and the relative concentrations [42], $1/(\theta_D^{\mathrm{FePt}})^3=(x/(\theta_D^{\mathrm{Fe}})^3)+(1-x)/(\theta_D^{\mathrm{Pt}})^3$. With these approximations it is then possible to estimate $\theta_E^{\mathrm{Si}}=522$ K and $\theta_E^{\mathrm{FePt}}=235$ K.

Young's modulus for FePt at room temperature, $E_{\mathrm{FePt}}=180$ GPa, has been recently reported by two different authors [41,43]. However, in those papers it was not mentioned how or where this value was obtained. Older measurements [44] in ordered alloys reported $E_{\mathrm{FePt}}=150$ GPa. Using the vibrating reed technique we measured a small piece of the FePt target used to fabricate the thin films and obtained $E_{\mathrm{FePt}}=165(10)$ GPa. X-ray diffraction and magnetization measurements confirmed that the target was in the ordered $L1_0$ phase. In the system FePd it is known that Young's modulus of disordered alloys is approximately 20% smaller [45] than in the ordered phase, which would give in our case $E_{\mathrm{FePt}}=130$ GPa at room temperature. In the same paper it was reported that the elastic constants increase by approximately 10% at 4 K (compared to the room temperature value) and our own measurements show a 6% decrease in E_{FePt} in the range 100–300 K. To account for the temperature variation of Young's modulus we used the empirical expression $E_{\mathrm{FePt}}(T)[\mathrm{GPa}]=142-T[\mathrm{K}]/25$.

The accepted value [34,41,43] for Poisson's ratio in FePt is $\nu=0.33$, and was assumed here to be independent of temperature. With Eqs. (2)–(4) we can calculate the temperature dependence of Q by considering the linear approximation for the strain and no dependence for the other parameters

$$Q(T)\simeq\frac{K_{\perp 0}-\frac{3}{2}\lambda(\alpha_s-\alpha_f)(T-T_0)E_{\mathrm{FePt}}/(1-\nu)}{2\pi M_s^2}, \tag{5}$$

or the full temperature dependence for all the involved variables

$$Q(T)\simeq\frac{K_{\perp 0}-\frac{3}{2}\lambda(T)\varepsilon(T)E_{\mathrm{FePt}}(T)/(1-\nu)}{2\pi M_s^2(T)}. \tag{6}$$

From all the parameters entering into Eq. (6) the dominant term (apart form the strain) is the quadratic dependence of $M_s(T)$ in the

denominator. The behavior of $M_s(T)$ was measured experimentally in a film of 94 nm, fitted with a power law and incorporated into Eq. (6) in order to calculate the variation of Q with temperature. Note that the magnetization enters in the expression of $Q(T)$ and also in the critical thickness, d_{cr} through the exchange length $d_l = \frac{1}{2}\sqrt{A(T)/(2\pi M_s^2(T))}$. In this last case d_l may be assumed to be independent of temperature due to the phenomenological relationship [46] $A(T) \propto M_s^2(T)$. The estimated value of the residual perpendicular anisotropy in these samples, $K_{\perp 0} = 1.5(4) \times 10^6$ erg/cm^3, has been already reported in Ref. [8].

Once the temperature dependence of $Q(T)$ is estimated, Eq. (1) can be used to obtain the variation of the critical thickness as a function of temperature. In Fig. 4 we show the calculated curves using the "linear" model, in which only the temperature variation of the thermal expansion was considered (Eq. (3)), and also the model that takes into account the temperature dependence of the parameters in Eq. (6) in the whole temperature range. These curves serve as a boundary to construct a phase diagram that defines regions of temperatures and thicknesses in which planar domains are separated from stripe domains by a coexistence line. As expected, when a reliable temperature dependence is used for $Q(T)$, the agreement between model and experiments is much better. Note that according to Eq. (6) and Fig. 5 the transition predicted from our model should occur at lower temperatures if the films are not uniformly stressed and that the estimated values of T_{sp} would be also smaller if this value is not taken from the maximum of H_c vs T curves. In any case the overall behavior is still well explained by the proposed model.

In the sample with $d = 94$ nm no transition is predicted and in fact this film shows a hysteresis loop that can be associated to a stripe domain structure in the whole temperature range. For this sample it is still possible to observe the influence of the interfacial induced strain on the magnetic behavior. A careful analysis of the loops of Fig. 2 at different temperatures shows that the in-plane saturation field decreases for decreasing temperatures. The temperature variation of this field is related with the Q-factor and the saturation magnetization through the relationship [8,18]

$$H_{S\parallel}(T) \sim 4\pi M_s Q\left(1 - \frac{1}{\sqrt{1+Q}}\frac{d_{cr}}{d}\right). \quad (7)$$

If the temperature dependence of M_s, Q, and d_{cr} is considered, Eq. (7) predicts a variation of $H_{S\parallel}(T)$ very similar to the measured experimental results, supporting the validity of our assumptions.

The model also predicts that for $d \leq 28$ nm the transition temperature between the two magnetic structures should be above room temperature. For example, using Eqs. (1) and (6) it is possible to estimate $T_{sp} \gtrsim 340$ K and $T_{sp} \gtrsim 420$ K for $d = 28$ nm and $d = 19$ nm, respectively. We made measurements for $T > 300$ K in the film with $d = 28$ nm and observed that the coercive field does not increase when increasing the temperature but decreases slightly. We also noted that if the hysteresis loop is remeasured at room temperature after heating the film, a smaller value of H_c is found. As mentioned in Refs. [7,9], it is not possible to perform magnetic measurements above room temperature without affecting the samples in an irreversible way, even if using relatively low temperatures. Our previous published results suggest that thermal energy favors the release of residual stresses and hence stabilize the configuration of planar domains. This reason helps to understand the absence of a maximum in H_c above room temperature in the samples with $d \leq 28$ nm.

4. Conclusions

By means of analyzing the temperature dependence of the coercive field we have shown that the magnetic domain configuration of disordered FePt films could be switched between in-plane domains and stripe domains by changing the temperature. The effect is observed for films in the range 35 nm $\leq d \leq 56$ nm and originates in the interfacial strain due to different thermal expansion coefficients of the Si substrate and the ferromagnetic alloy. In thicker films ($d > 56$ nm) the change in Q is not enough to eliminate the stripe structure and the absence of a transition also occurs in thinner films ($d \leq 28$ nm) in which T_{sp} is predicted to occur above room temperature. All these results could be reasonably well explained by considering an expression for the full temperature dependence of the thermal induced stress which produces an anisotropy axis perpendicular to the film plane. To obtain a better fit of the experiments it would be very useful to have reliable data for the thermal expansion coefficient, the magnetostriction constant and Poisson's ratio of FePt alloys as a function of temperature, both in the ordered and the disordered states.

Acknowledgments

This was supported in part by Conicet under Grant PIP 112-200801-00245, ANPCyT Grant PICT 2010-0773, and U.N. Cuyo Grant 06/C352, all from Argentina. Technical support from Rubén E. Benavides and Matías Guillén is deeply acknowledged.

References

[1] S. Okamoto, N. Kikuchi, O. Kitakami, T. Miyazaki, Y. Shimada, K. Fukamichi, Physical Review B 66 (2002) 024413.
[2] K.R. Coffey, M.A. Parker, J.K. Howard, IEEE Transactions on Magnetics 31 (1995) 2737.
[3] R.A. Ristau, K. Barmak, L.H. Lewis, K.R. Coffey, J.K. Howard, Journal of Applied Physics 86 (1999) 4527.
[4] S. Jeong, Y.-H. Hsu, D.E. Laughlin, M.E. McHenry, IEEE Transactions on Magnetics 37 (2001) 1299.
[5] R.F.C. Farrow, D. Weller, R.F. Marks, M.F. Toney, S. Hom, G.R. Harp, A. Cebollada, Applied Physics Letters 69 (1996) 1166.
[6] M. Vásquez Mansilla, J. Gómez, A. Butera, IEEE Transactions on Magnetics 44 (2008) 2883.
[7] M. Vásquez Mansilla, J. Gómez, E. Sallica Leva, F. Castillo Gamarra, A. Asenjo Barahona, A. Butera, Journal of Magnetism and Magnetic Materials 321 (2009) 2941.
[8] E. Sallica Leva, R.C. Valente, F. Martínez Tabares, M. Vásquez Mansilla, S. Roshdestwensky, A. Butera, Physical Review B 82 (2010) 144410.
[9] E. Burgos, E. Sallica Leva, J. Gómez, F. Martínez Tabares, M. Vásquez Mansilla, A. Butera, Physical Review B 83 (2011) 174417.
[10] D.M. Jacobi, E. Sallica Leva, N. Álvarez, M. Vásquez Mansilla, J. Gómez, A. Butera, Journal of Applied Physics 111 (2012) 033911.
[11] M. Hehn, S. Padovani, K. Ounadjela, J.P. Bucher, Physical Review B 54 (1996) 3428.
[12] V. Gehanno, Y. Samson, A. Marty, B. Gilles, A. Chamberod, Journal of Magnetism and Magnetic Materials 172 (1997) 26.
[13] A. Asenjo, J.M. García, D. García, A. Hernando, M. Vázquez, P.A. Caro, D. Ravelosona, A. Cebollada, A. Briones, Journal of Magnetism and Magnetic Materials 196 (1999) 23.
[14] L. Folks, U. Ebels, R. Soorykumar, D. Weller, R.F.C. Farrow, Journal of the Magnetics Society of Japan 23 (S1) (1999) 85.
[15] R. Bručas, H. Hafermann, M.I. Katsnelson, I.L. Soroka, O. Eriksson, B. Hjörvarsson, Physical Review B 69 (2004) 064411.
[16] C.A. Ramos, E. Vassallo Brigneti, J. Gómez, A. Butera, Physica B 404 (2009) 2784.
[17] A. Hubert, R. Schäfer, Magnetic Domains, 3rd edition, Springer, 2009.
[18] Y. Murayama, Journal of the Physical Society of Japan 21 (1966) 2253.
[19] A.L. Sukstanskii, K.I. Primak, Journal of Magnetism and Magnetic Materials 169 (1997) 31.
[20] V. Gehanno, R. Hoffmann, Y. Samson, A. Marty, S. Auffret, European Physical Journal B 10 (1999) 457.
[21] N. Álvarez, J. Gómez, A. Butera, unpublished.
[22] S. Okamoto, O. Kitakami, N. Kikuchi, T. Miyazaki, Y. Shimada, Y.K. Takahashi, Physical Review B 67 (2003) 094422.
[23] T. Bublat, D. Goll, Journal of Applied Physics 108 (2010) 113910.
[24] P. Sharma, N. Kaushik, A. Makino, A. Inoue, IEEE Transactions on Magnetics 47 (2011) 4394.
[25] B.D. Cullity, C.D. Graham, Introduction to Magnetic Materials, 2nd edition, Wiley, New Jersey, 2009.
[26] P. Gaunt, Philosophical Magazine Part B 48 (1983) 261.
[27] X. Chen, P. Gaunt, Journal of Applied Physics 65 (1989) 3980.
[28] H. Kronmüller, K.-D. Durst, M. Sagawa, Journal of Magnetism and Magnetic Materials 74 (1988) 291.

[29] A. Butera, J.L. Weston, J.A. Barnard, IEEE Transactions on Magnetics 34 (1998) 1024.
[30] X. Guo, X. Chen, Z. Altounian, J.O. Ström-Olsen, Journal of Applied Physics 73 (1993) 6275.
[31] T.W. Kim, R.J. Gambino, Journal of Applied Physics 81 (1997) 5184.
[32] P. Zou, W. Yu, J.A. Bain, IEEE Transactions on Magnetics 38 (2002) 3501.
[33] J.A. Aboaf, T.R. McGuire, S.R. Herd, E. Klokholm, IEEE Transactions on Magnetics 20 (1984) 1642.
[34] F.E. Spada, F.T. Parker, C.L. Platt, J.K. Howard, Journal of Applied Physics 94 (2003) 5123.
[35] H. Shima, K. Oikawa, A. Fujita, K. Fukamichi, K. Ishida, Journal of Magnetism and Magnetic Materials 272–276 (2004) 2173.
[36] W. Wunderlich, K. Takahashi, D. Kubo, Y. Matsumara, Y. Nishi, Journal of Alloys and Compounds 475 (2009) 339.
[37] J.E. Schmidt, L. Berger, Journal of Applied Physics 55 (1984) 1073.
[38] S. Tamulevičius, Vacuum 51 (1998) 127.
[39] C.V. Thompson, R. Carel, Journal of the Mechanics and Physics of Solids 44 (1996) 657.
[40] D. Sander, Reports on Progress in Physics 62 (1999) 809.
[41] P. Rasmussen, X. Rui, J.E. Shield, Applied Physics Letters 86 (2005) 191915.
[42] G.B. Mitra, T. Chattopadhyay, Acta Crystallographica A 28 (1972) 179.
[43] S.N. Hsiao, F.T. Huan, H.W. Chang, H.W. Huang, S.K. Chen, H.Y. Lee, Applied Physics Letters 94 (2009) 232505.
[44] H. Masumoto, T. Kobayashi, Transactions of the Japan Institute of Metals 6 (1965) 113.
[45] T. Ichitsubo, K. Tanaka, Journal of Applied Physics 96 (2004) 6200.
[46] H. Kronmuller, M. Fahnie, Micromagnetism and the Microstructure of Ferromagnetic Solids, Cambridge University Press, Cambridge, 2003.